Relating the multi-angle quantum approximate optimization algorithm and continuous-time quantum walks on dynamic graphs

Rebekah Herrman*
Department of Industrial and Systems Engineering
University of Tennessee at Knoxville
Knoxville, TN 37996 USA

In this work, we show that ma-QAOA is equivalent to a restriction of continuous-time quantum walks on dynamic graphs. We then show it is universal for computation by finding the appropriate B and C operators and angles that implement the universal gate set consisting of the Hadamard, $\pi/8$ and Controlled-Not gates in the ma-QAOA framework. This result begins to bridge the gap between the continuous-time quantum walk model and gate model of quantum computation.

I. INTRODUCTION

In classical computing, combinatorial optimization (CO) problems are defined by bits and constraints on the bits, called clauses. The goal of these problems is to maximize or minimize some objective,

$$C = \sum_a C_a,$$

where C_a refers to the ath clause. The quantum approximate optimization algorithm (QAOA) is a well-studied algorithm that approximately solves CO problems [1]. The algorithm requires that C is encoded into a unitary operator

$$U(\gamma, C) = e^{-iC\gamma},$$

where $\gamma \in \mathbb{R}$ is a real valued parameter, often called an angle. $U(\gamma, C)$ and a mixing unitary,

$$U(\beta, B) = e^{-iB\beta}$$

where $\beta \in \mathbb{R}$, are applied to an initial state which is the equal superposition over the computational basis states

$$|s\rangle = \frac{1}{\sqrt{2^n}} \sum_z |z\rangle.$$

Typically B is a sum of Pauli-x operators acting on each qubit, however, other mixers have been considered [2, 3]. The QAOA ansatz applied p times to $|s\rangle$ is denoted p-QAOA. The result of p-QAOA is

$$|\gamma, \beta\rangle = U(\beta_p, B)U(\gamma_p, C)\dots U(\beta_1, B)U(\gamma_1, C)|s\rangle,$$

where the subscript i denotes the angle chosen for iteration i of the algorithm. The classical parameters γ and β are chosen to maximize $\langle \gamma, \beta | C | \gamma, \beta \rangle$. While QAOA is typically thought of as an algorithm that solves CO problems, it has been shown to be a universal model of quantum computation [4, 5]. Recently, multi-angle QAOA (ma-QAOA) was introduced as a generalization of QAOA that allows for additional classical parameters [6]. In that same paper, it was shown that ma-QAOA always performs at least as well as QAOA for optimization and can strictly outperform it in some cases.

Continuous-time quantum walks on dynamic graphs (dynamic CTQWs) were introduced in [7] and proven to be universal for quantum computation. In this paper, we show that ma-QAOA is equivalent to a restriction of dynamic CTQWs in Section II. We then find the appropriate operators B and C, and angles β and γ that implement the universal gate set of the Hadamard (H), $\pi/8$ (T), and Controlled-Not (CX) gates in Section III. These gates have been determined in the dynamic CTQW framework, so the graphs and times used in that framework define the operators and angles used in the ma-QAOA framework. In Section IV, we work through the implementation of the H, T and CX gates and then close with a discussion in Section V.

---

* rherrma2@utk.edu

II.   BACKGROUND

In this section, we present relevant background information for ma-QAOA and dynamic CTQWs. We then discuss how ma-QAOA can be viewed as a restriction of dynamic CTQWs.

A.   ma-QAOA

Multi-angle QAOA is a generalization of QAOA in which additional classical parameter input are allowed. As with QAOA, in ma-QAOA two operators $U(\vec{\gamma_\ell}, C)$ and $U(\vec{\beta_\ell}, B)$ are applied in succession to the state $|s\rangle$ which is an equal superposition over the computational basis. $U(\vec{\gamma_\ell}, C)$ and $U(\vec{\beta_\ell}, B)$ are defined as

$$U(\vec{\gamma_\ell}, C) = e^{-i \sum_a C_a \gamma_{\ell,a}} = \prod_a e^{-i\gamma_{\ell,a} C_a}$$

and

$$U(\vec{\beta_\ell}, B) = e^{-i \sum_{v \in V(G)} B_v \beta_{\ell,v}} = \prod_{v \in V(G)} e^{-i\beta_{\ell,v} B_v}.$$

Here, $\vec{\gamma_\ell} = (\gamma_{\ell,a_1}, \gamma_{\ell,a_2}, \ldots, \gamma_{\ell,a_m}) \in \mathbb{R}^m$ is the vector of angles used when $U(\vec{\gamma_\ell}, C)$ is applied for the ℓth time and $\vec{\beta_\ell} = (\beta_{\ell,v_1}, \beta_{\ell,v_2}, \ldots, \beta_{\ell,v_n}) \in \mathbb{R}^n$ is the vector of β angles for $U(\vec{\beta_\ell}, B)$ when applied for the ℓth time. Each a denotes a clause in the CO problem and v_j refers to a specific qubit in the problem formulation, and B_v typically refers to the Pauli-x matrix acting on qubit v. Each problem can be translated into a graph by identifying each qubit with a vertex and each interaction between qubits with an edge between the appropriate vertices [8–10].

Typically, C is identified with a combinatorial optimization problem, such as MaxCut. The objective function for the MaxCut problem is

$$\min_{x \in \{0,1\}^n} \sum_{ij \in E(G)} x_j(x_i - 1) + x_i(x_j - 1) = \min_{x \in \{0,1\}^n} \sum_{ij \in E(G)} 2x_i x_j - x_i - x_j.$$

This is encoded into C as

$$C = 1/2 \sum_{ij \in E(G)} (-Z_i Z_j + I)$$

where Z_j is the Pauli-z operator acting on qubit j and I is the $2^n \times 2^n$ identity matrix. This is a diagonal matrix, so we denote the diagonal entries $d_0, \ldots, d_{2^n-1}$. Note that all entries of C are zero except for possibly the diagonal entries d_1 through d_{2^n-2}, depending on the edges in the graph.

B.   Dynamic CTQWs

Continuous-time quantum walks (CTQWs) on graphs were introduced to search decision trees [11] and have numerous applications including modeling coherent transport on complex networks [12] and spatial searches [13]. Furthermore, they are universal for computation [14]. In a CTQW on a graph $G = (V, E)$, a walker moves between vertices of G according to the Schrödinger equation

$$i\frac{d|\psi\rangle}{dt} = H|\psi\rangle,$$

where $\hbar = 1$, and H is either equal to the adjacency matrix or Laplacian of G. In this work, we use the adjacency matrix formulation.

The concept of CTQWs on dynamic graphs was introduced in [7] and proven to be universal for computation. A dynamic CTQW is a set of continuous-time quantum walks on a *dynamic graph*. A dynamic graph is a set of ordered pairs of graphs and associated propagation times, $\mathcal{G} = \{(G_i, t_i)\}$. A dynamic CTQW is defined to be a sequence of
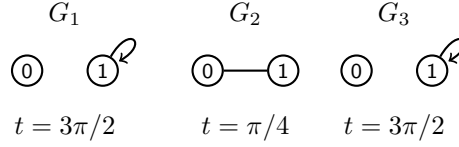
$$G_1 \qquad\qquad G_2 \qquad\quad G_3$$

$$t = 3\pi/2 \qquad t = \pi/4 \qquad t = 3\pi/2$$

FIG. 1: The dynamic CTQW implementation of the H gate, which requires three graphs, G_1, G_2, and G_3.
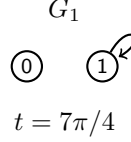
$$G_1$$

$$t = 7\pi/4$$

FIG. 2: The dynamic CTQW implementation of the T gate.

CTQWs on each graph G_i for the associated time t_i performed in order of increasing index on some initial state. Mathematically, let $|\psi_0\rangle$ be the initial state of the walker and $\{(G_1, t_1), (G_2, t_2), \ldots, (G_k, t_k)\}$ be the dynamic CTQW that acts upon it. Then the final state of the walker, $|\psi\rangle$, is

$$|\psi\rangle = e^{-iA_k t_k/||A_k||} \ldots e^{-iA_2 t_2/||A_2||} e^{-iA_1 t_1/||A_1||} |\psi_0\rangle$$

where A_i is the adjacency matrix of G_i and $||A_i||$ is the spectral norm of A_i.

When showing dynamic CTQWs were universal for computation, the authors of [7] defined each G_i to have 2^n vertices, which is the number of possible states in an n-qubit system. The vertices of these graphs were allowed to have self-loops, which adds phase to the quantum state, however multi-edges were not permitted. A self-loop in the dynamic graph on vertex v is represented in the adjacency matrix as a 1 on the diagonal element d_v. In the original dynamic CTQW formulation, any vertex that did not have an edge incident to it was required to have a self-loop, however the author of [15] relaxed this condition so that vertices can exist in isolation without accumulating phase. We will use this relaxation throughout this paper.

We now recall the dynamic CTQWs that give the universal gate set of H, T, and CX as defined in [15].

1. Dynamic CTQW implementation of the H gate

The dynamic CTQW equivalent of the single qubit H gate consists of three graphs [15] which are shown in Figure 1. Formally, the dynamic CTQW for this gate is written as $\mathcal{G}_H = \{(G_1, 3\pi/2), (G_2, \pi/4), (G_3, 3\pi/2)\}$, and the adjacency matrices corresponding to G_1, G_2, and G_3 are A_1, A_2, and A_3, respectively. These adjacency matrices are

$$A_1 = A_3 = \begin{pmatrix} 0 & 0 \\ 0 & 1 \end{pmatrix} \quad A_2 = \begin{pmatrix} 0 & 1 \\ 1 & 0 \end{pmatrix}.$$
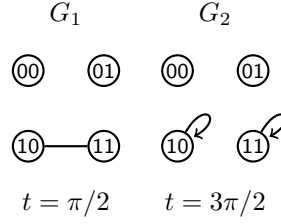
2. Dynamic CTQW implementation of the T gate

The dynamic CTQW equivalent of the T gate consists of a single graph [15], which is shown in Figure 2. The dynamic CTQW for this gate is written as $\mathcal{G}_T = \{(G_1, 7\pi/4)\}$, and the adjacency matrix corresponding to G_1 is

$$A_1 = \begin{pmatrix} 0 & 0 \\ 0 & 1 \end{pmatrix}.$$

3. Dynamic CTQW implementation of the CX gate

The dynamic CTQW equivalent of the two qubit CX gate consists of two graphs [15] which are shown in Figure 3. Formally, the dynamic CTQW for this gate is written as $\mathcal{G}_{CX} = \{(G_1, \pi/2), (G_2, 3\pi/2)\}$, and the adjacency matrices corresponding to G_1 and G_2 are A_1 and A_2, respectively. These adjacency matrices are

FIG. 3: The dynamic CTQW implementation of the CX gate, which requires two graphs, G_1 and G_2.

$$A_1 = \begin{pmatrix} 0 & 0 & 0 & 0 \\ 0 & 0 & 0 & 0 \\ 0 & 0 & 0 & 1 \\ 0 & 0 & 1 & 0 \end{pmatrix} \quad A_2 = \begin{pmatrix} 0 & 0 & 0 & 0 \\ 0 & 0 & 0 & 0 \\ 0 & 0 & 1 & 0 \\ 0 & 0 & 0 & 1 \end{pmatrix}.$$

C. ma-QAOA as a restriction of dynamic CTQWs

Both ma-QAOA and dynamic CTQWs act on an initial state $|\psi\rangle$ by applying operators of the form $e^{-iA_j t_j}$ where A_j is a Hermitian matrix and t_j is a real valued parameter. Both methods use underlying graphs to determine the structure of A_j, as well. Furthermore, all dynamic CTQWs for the gate set H, T, and CX consist of alternating a graph that has self-loops as its only edges with graphs that have no self-loops as edges. Multi-angle QAOA is similar in that the C matrix contains only diagonal entries, which is the adjacency matrix of a graph with only self-loops, up to constants, while the B matrix has only off-diagonal positions. The main difference is that in ma-QAOA, the two operators B and C have well-defined structure that does not change with the number of iterations of the algorithm. In contrast, the dynamic CTQW graphs have no such restriction.

Thus, it is natural to think of ma-QAOA as a restriction of dynamic CTQWs where alternate graphs have adjacency matrix C and the others have adjacency matrix B. In order to explicitly relate ma-QAOA to dynamic CTQWs, one can define the ma-QAOA C matrix as a sum of matrices, $\sum_a C_a$, each of which receives its own angle γ_a. One can also define a $B = \sum_d B_d$ matrix as a sum of matrices that receives its own angle β_d. If $\sum C_a \gamma_a = A_k t_k$, then $e^{-i \sum_a C_a \gamma_a} = e^{-iA_k t_k}$, so $U(\gamma, C)$ acts on a quantum state the same way that $e^{-iA_k t_k}$ does, which clearly holds when considering $\sum_d B_d$ and β_d, as well. Thus, we can show that ma-QAOA is universal for computation if we can develop B and C matrices and find appropriate $\vec{\beta}$ and $\vec{\gamma}$ such that $\sum B_d \beta_d = A_k t_k$ or $\sum C_a \gamma_a = A_k t_k$ for each graph A_k and associated time t_k in the dynamic CTQW representation of the H, T, and CX gates.

When implementing the dynamic CTQWs, there are two types of graphs- graphs in which a subset of vertices has self-loops with no other edges, and graphs that contain only edges with no self-loops. When solving the MaxCut problem with ma-QAOA, C is a diagonal matrix with non-negative entries, which can be seen as the adjacency matrix of a graph with only weighted self-loops. B has only off-diagonal entries that are 0-1 valued, which can be seen as the adjacency matrix of a graph with no self-loops.

Since C is a diagonal matrix, we want to relate C to the dynamic CTQW matrices that have only self-loops as edges. The first and last adjacency matrices in the dynamic CTQW implementation of the H gate, the only matrix in the dynamic CTQW implementation of the T gate, and the last matrix in the dynamic CTQW implementation of the CX gate are the only matrices that satisfy these criteria. Note that the self-loops for these graphs do not necessarily appear on the same vertices, so when defining C, we require that an arbitrary diagonal position of C is the only non-zero entry of C. Thus, we want to define C such that there exists a collection of angles γ_a associated with each C_a such that $e^{-i \sum_a C_a \gamma_a} = e^{-iA_k t_k}$ where A_k is an arbitrary diagonal matrix.

Similarly, one can define a B matrix as a sum of matrices, $\sum_d B_d$, each of which receives its own angle, β_d. We want to relate B to the dynamic CTQW graphs that do not contain self-loops, which are the second graph in the H gate implementation and the first graph in the CX gate implementation. Thus, we want to define B such that there exists a collection of angles β_d associated with each B_d such that $e^{-i \sum_d B_d \beta_d} = e^{-iA_k t_k}$ where A_k is a matrix of the form used in the dynamic CTQW implementation of the H and CX gates. An advantage of relating ma-QAOA to dynamic CTQWs is that well-studied CTQW phenomena, such as hitting times, could potentially be used to understand ma-QAOA better and could potentially be used to find optimal ma-QAOA β parameters.

III.   USING MA-QAOA TO IMPLEMENT A UNIVERSAL GATE SET

In this section, we show how the ma-QAOA operators B and C and parameters $\vec{\beta}$ and $\vec{\gamma}$ can be selected that implement the equivalent of the dynamic CTQW universal set of gates H, T, and CX.

A.   Defining C

First, we discuss how to define the C operator. In the dynamic CTQW formulation, phase can be added to arbitrary vertices in the graph. The MaxCut C formulation in Section II A, however, does not allow for this; for example, since the diagonal entries corresponding to $|0 \dots 0\rangle$ and $|1 \dots 1\rangle$ are always 0, no phase can ever be added to these vertices. Thus, the MaxCut definition of C from Section II A is not sufficient to implement the universal gate set. In order to ensure that phase can be added to any vertex, we modify C to obtain

$$C = \sum_z |z\rangle\langle z|.$$

In terms of the operators from Section II A, each clause C_a is defined as $C_a = |a\rangle\langle a|$. The following property of C is needed to implement the universal gate set H, T, and CX.

Property III.1. Let z be a base-10 number and $z_0 \dots z_{n-1}$ its binary representation. There exists a linear combination of summands of C with coefficients in $\{0, 1\}$ and the only non-zero diagonal entry of the linear combination is in position z.

Proof. By definition, $|z\rangle = |z_0\rangle \otimes \dots \otimes |z_{n-1}\rangle$, and $|z_i\rangle\langle z_i| = ((-1)^{z_i} Z_i + I_i)/2$ for $z_i \in \{0, 1\}$, as

$$(Z_i + I_i)/2 = [|0\rangle\langle 0| + |1\rangle\langle 1| + (|0\rangle\langle 0| - |1\rangle\langle 1|)]/2 = |0\rangle\langle 0|$$

and

$$(-Z_i + I_i)/2 = [|0\rangle\langle 0| + |1\rangle\langle 1| - (|0\rangle\langle 0| - |1\rangle\langle 1|)]/2 = |1\rangle\langle 1|.$$

If vertex z is the only vertex to receives phase, then C_z receives a coefficient of 1, while all other summands of C receive a coefficient of 0. This ensures that z is the only non-zero entry of the linear combination. $\square$
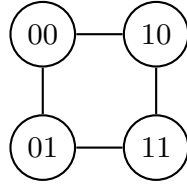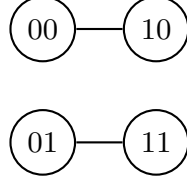
Thus, phase can be added to an arbitrary vertex by picking the appropriate linear combination of summands of C. One potential drawback to this formulation of C is that all combinations of Z gates are required, which can lead to deep circuits. However, the diffusion operation in Grover's algorithm uses Z gates and can be implemented in a scalable manner [16], so we expect that the above C can be implemented on large systems, as well.

B.   Defining B

We now turn our attention to defining B. The T gate requires only self-loops, so it does not need to be considered when developing the B matrix. The B matrix requires summands such that a linear combination of the summands results in the adjacency matrix of a discrete hypercube, which is needed to implement the H gate. In order to implement a CX gate using B, a linear combination of the summands must also result in non-zero entries at positions (a, b) and (b, a) such that the binary representations of a and b have a 1 in position j and the binary representations of a and b are identical except in position v. This must be possible for all choices of j and v.

In order to begin constructing B, first note that the sum of all Pauli-x matrices acting on a single qubit, $\sum_i X_i$, is a matrix that is identical to the adjacency matrix of the discrete hypercube graph. Thus, we include $\sum_i X_i$ in the definition of B. Unfortunately, CX is not easily implemented with just X_i. Each X_i term connects vertices that contain a 0 in position i in its binary representation to a vertex that contains 1 in position i in its binary representation, where the rest of the terms in the binary representation are identical. For example, consider a two qubit system. Let $B = X_1 + X_2$, where X_i is the Pauli-x operator acting on qubit i. Then

$$B = \begin{pmatrix} 0 & 1 & 1 & 0 \\ 1 & 0 & 0 & 1 \\ 1 & 0 & 0 & 1 \\ 0 & 1 & 1 & 0 \end{pmatrix}.$$

FIG. 4: The graph given by the adjacency matrix $B = X_1 + X_2$.

FIG. 5: The graph given by the adjacency matrix $B = X_1$.

This is the adjacency matrix of the graph in Figure 4. If $B = X_1$, then

$$B = \begin{pmatrix} 0 & 0 & 1 & 0 \\ 0 & 0 & 0 & 1 \\ 1 & 0 & 0 & 0 \\ 0 & 1 & 0 & 0 \end{pmatrix},$$

which is the adjacency matrix for the graph in Figure 5. In fact, if B has a summand X_i, then it is the adjacency matrix for a graph in which the vertex corresponding to $|0\ldots0\rangle$ is adjacent to some other vertex in the graph. However, $|0\ldots0\rangle$ will never be affected by a CX gate. Thus, we require a method that removes any edge incident to $|0\ldots0\rangle$, and potentially other edges that are not used in the CX gate.

One method of eliminating these edges is to subtract terms of the form $X_i Z_j$ to X_i. For example, if $B = X_1 - X_1 Z_2$, then

$$B = \begin{pmatrix} 0 & 0 & 0 & 0 \\ 0 & 0 & 0 & 2 \\ 0 & 0 & 0 & 0 \\ 0 & 2 & 0 & 0 \end{pmatrix}.$$
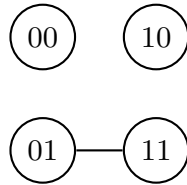
When divided by two, this gives the adjacency matrix of the graph in Figure 6, which connects vertices that are swapped in a CX with control bit 2 and target bit 1.

We will now show that B of the form

$$B = 1/2 (\sum_v X_v - \sum_v \sum_{j \neq v} X_v Z_j),$$

has the following property that will be needed to implement the CX gate.

Property III.2. There exists a linear combination of summands of B, called B', with coefficients in $\{0, 1\}$ such that for arbitrary qubits $1 \leq v \leq n$ and $1 \leq j \leq n$ where $v \neq j$, $B' = |0_v 1_j\rangle\langle 1_v 1_j| + |1_v 1_j\rangle\langle 0_v 1_j|$.

FIG. 6: The graph given by the adjacency matrix $B = X_1 - X_1 Z_2$.

Proof. Let us show that $1/2(X_j - X_j Z_v)$ yields a matrix with the above property.

$$
\begin{aligned}
(X_v - X_v Z_j) &= (|0_v\rangle\langle 1_v| + |1_v\rangle\langle 0_v|) - [(|0_v\rangle\langle 1_v| + |1_v\rangle\langle 0_v|) \otimes (|0_j\rangle\langle 0_j| - |1_j\rangle\langle 1_j|)] \\
&= (|0_v\rangle\langle 1_v| + |1_v\rangle\langle 0_v|) \otimes (|0_j\rangle\langle 0_j| + |1_j\rangle\langle 1_j| - (|0_j\rangle\langle 0_j| - |1_j\rangle\langle 1_j|)) \\
&= (|0_v\rangle\langle 1_v| + |1_v\rangle\langle 0_v|) \otimes 2|1_j\rangle\langle 1_j| \\
&= 2(|0_v 1_j\rangle\langle 1_v 1_j| + |1_v 1_j\rangle\langle 0_v 1_j|).
\end{aligned}
$$

Dividing by two gives the result. $\qquad\square$

C. Selecting $\vec{\beta}$ and $\vec{\gamma}$ for the H gate

The Hadamard gate, H, acts on a single qubit and can be represented by the matrix

$$
H = \frac{1}{\sqrt{2}} \begin{pmatrix} 1 & 1 \\ 1 & -1 \end{pmatrix}.
$$

The authors of [17] showed that the $H^{\otimes n}$ gate can be implemented in the dynamic CTQW framework using a sequence consisting of self-loops, an n-dimensional hypercube, and more self-loops. The self loops can be implemented by the C operators described earlier in this section and are used to add phase ω_v to vertex v based on its Hamming distance from $|0\dots0\rangle$. Let $h(v)$ be the Hamming distance of vertex v relative to $|0\dots0\rangle$. The phase factor required to implement the H gate is

$$
\omega_v = \begin{cases} -1, & h(v) \cong 0 \pmod 4 \\ -i, & h(v) \cong 1 \pmod 4 \\ 1, & h(v) \cong 2 \pmod 4 \\ i, & h(v) \cong 3 \pmod 4 \end{cases}
$$

which is derived in [17]. Since $||C_i|| = 1$ for all i, the angles required to obtain the above phases are $\vec{\gamma_1} = \vec{\eta} = (\eta_1, \dots)$, where η_v is

$$
\eta_v = \begin{cases} \pi, & h(v) \cong 0 \pmod 4 \\ \pi/2, & h(v) \cong 1 \pmod 4 \\ 0, & h(v) \cong 2 \pmod 4 \\ 3\pi/2, & h(v) \cong 3 \pmod 4. \end{cases}
$$

The B operator defined earlier in this section can be used to implement the n-dimensional hypercube. For the n-dimensional hypercube, we set all $\vec{\beta_1} = (n\pi/4, \dots, n\pi/4, 0, \dots, 0)$, where all $n\pi/4$ angles correspond to X_i terms in the sum and all 0 angles correspond to terms of the form $X_i Z_j$. Note that $n\pi/4$ is the dynamic CTQW hypercube mixing time for the H gate. For the last self-loop graph, we let $\vec{\gamma_2} = \vec{\gamma_1}$.

D. Selecting $\vec{\beta}$ and $\vec{\gamma}$ for the T gate

The T gate acts on a single qubit and is represented by the matrix

$$
T = \begin{pmatrix} 1 & 0 \\ 0 & e^{\frac{i\pi}{4}} \end{pmatrix}
$$

The T gate acting on qubit k adds a phase to all vertices that have a 1 in position k in their binary representation. This can be implemented by finding the linear combinations of summands of C that give non-zero d_i where d_i has a 1 in position k of its binary representation and setting $\gamma_i = 7\pi/4$, since $-7\pi/4 = \pi/4$, while setting the rest of the γ_j to 0. Note that in order to implement this single qubit gate with ma-QAOA, we use C_a, which depends on multi-qubit interactions. This is because C must be able to add self-loops to arbitrary vertices in order to implement the H gate, and C is not allowed to change from iteration to iteration of ma-QAOA.
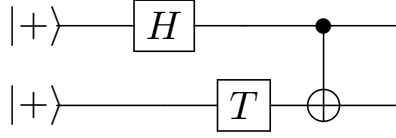
FIG. 7: The example circuit.

U	Angle vector
$U(\gamma_1, C)$	$(\pi, \pi, \pi/2, \pi/2)$
$U(\beta_1, B)$	$(0, \pi/4, \pi/4, 0)$
$U(\gamma_2, C)$	$(\pi, \pi, \pi/2, \pi/2)$
$U(\beta_2, B)$	$(0, 0, 0, 0)$
$U(\gamma_3, C)$	$(0, 7\pi/4, 0, 7\pi/4)$
$U(\beta_3, B)$	$(0, 0, 0, 3\pi/2)$
$U(\gamma_4, C)$	$(0, 0, \pi/2, \pi/2)$
$U(\beta_4, B)$	$(0, 0, 0, 0)$

TABLE I: The $\beta_{p,i-j}$ angles for an ma-QAOA implementation of the circuit found in Figure 7. The vectors γ_i have entries $(\gamma_{i,0}, \gamma_{i,1}, \gamma_{i,2}, \gamma_{i,3})$ and vectors β_j have entries $(\beta_{j,0-1}, \beta_{j,0-2}, \beta_{j,1-3}, \beta_{j,2-3})$, where the subscript $f - g$ for $f, g \in \mathbb{R}$ refers to the edge connecting vertex f to vertex g.

E.   Selecting $\vec{\beta}$ and $\vec{\gamma}$ for the CX gate

The controlled-not gate, denoted CX, is a two qubit gate. The matrix representation when the control is the first qubit and the target is the second qubit is

$$CX = \begin{pmatrix} 1 & 0 & 0 & 0 \\ 0 & 1 & 0 & 0 \\ 0 & 0 & 0 & 1 \\ 0 & 0 & 1 & 0 \end{pmatrix}.$$

The dynamic CTQW for this gate is easy to implement and requires one graph that adds phase to a subset of vertices and another which connects vertices based on which bit is the control and which is the target. These two graphs can be performed in any order. Property III.1 and Property III.2 can be used to implement the CX gate with ma-QAOA, and the implementation is similar to the dynamic CTQW one. From Property III.2, $e^{-i(X_j - X_j Z_v)\pi/2}$ gives the adjacency matrix for the CX gate with control bit v and target bit j, up to a factor of $-i$ on the qubits affected by the swap. The $-i$ factor is eliminated by adding a phase of i to the vertices affected by the swap via Property III.1.

IV.   EXAMPLE

Let us examine the circuit in Figure 7. It has two qubits and an H gate acts on the first qubit, a T on the second, and a CX targets the second qubit and is controlled by the first. This will require 4 layers of ma-QAOA. The angles that implement this circuit with ma-QAOA are found in Table I.

We now confirm that these angles implement the above circuit when used with the B and C operators as defined above. First, note that $H \otimes I$ followed by $I \otimes T$ followed by CX with control qubit 1 and target qubit 2 acts on the state $|+\rangle$ as

$$1/2\big[|00\rangle + |01\rangle + |10\rangle + |11\rangle\big]$$
$$\xrightarrow{H \otimes I} 1/\sqrt{2}\big[|00\rangle + |01\rangle\big] + 0\big[|10\rangle + |11\rangle\big]$$
$$\xrightarrow{I \otimes T} 1/\sqrt{2}\big[|00\rangle + e^{i\pi/4}|01\rangle\big] + 0\big[|10\rangle + e^{i\pi/4}|11\rangle\big]$$
$$\xrightarrow{CX} 1/\sqrt{2}\big[|00\rangle + e^{i\pi/4}|11\rangle\big] + 0\big[e^{i\pi/4}|01\rangle + |10\rangle\big]$$

$$U(\vec{\gamma}_1, C) \qquad U(\vec{\beta}_1, B) \qquad U(\vec{\gamma}_2, C) \qquad U(\vec{\beta}_2, B)$$

$$U(\vec{\gamma}_3, C) \qquad U(\vec{\beta}_3, B) \qquad U(\vec{\gamma}_4, C) \qquad U(\vec{\beta}_4, B)$$
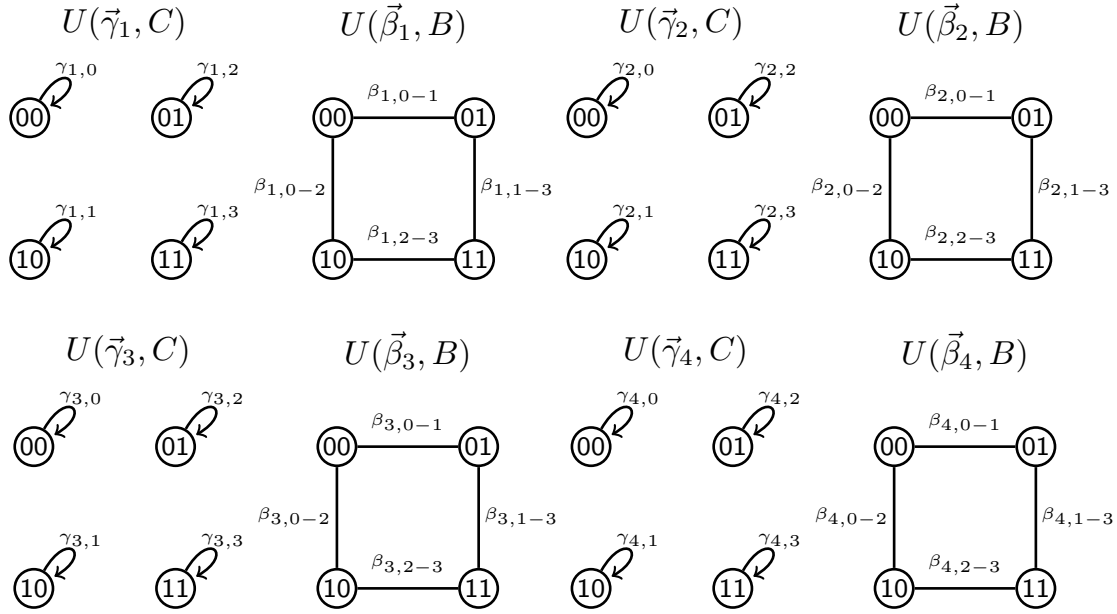
FIG. 8: The ma-QAOA implementation of the circuit found in Figure 7 with angles found in Table I. The top row implements the H gate, the left graph on the bottom row implements the T gate, and the bottom middle two graphs implement the CX gate. The last graph is not necessary, but is included to show four full iterations of ma-QAOA.

The ma-QAOA implementation of the H gate varies slightly from above, as H only acts on one qubit in this circuit, not both of them. The 1-dimensional hypercube is a path on two vertices, and since the H is performed on the first qubit, the non-zero β angles correspond to edges that connect vertices whose first qubit are either both 0 or both 1. Additionally, the ω_v are changed so that one vertex in each two-dimensional hypercube has a factor of -1 and the other has a factor of $-i$. The angles for this implementation are found in Table I. These angles act on the initial state $|+\rangle$ as

$$1/2\big[|00\rangle + |01\rangle + |10\rangle + |11\rangle\big]$$
$$\xrightarrow{U(\vec{\gamma_1},C)} -1/2\big[|00\rangle + |01\rangle\big] - i/2\big[|10\rangle + |11\rangle\big]$$
$$\xrightarrow{U(\vec{\beta_1},B)} -1/\sqrt{2}\big[|00\rangle + |01\rangle\big] + 0\big[|10\rangle + |11\rangle\big]$$
$$\xrightarrow{U(\vec{\gamma_2},C)} 1/\sqrt{2}\big[|00\rangle + |01\rangle\big] + 0\big[|10\rangle + |11\rangle\big]$$
$$\xrightarrow{U(\vec{\gamma_2},B)} 1/\sqrt{2}\big[|00\rangle + |01\rangle\big] + 0\big[|10\rangle + |11\rangle\big]$$
$$\xrightarrow{U(\vec{\gamma_3},C)} 1/\sqrt{2}\big[|00\rangle + e^{i\pi/4}|01\rangle\big] + 0\big[|10\rangle + e^{i\pi/4}|11\rangle\big]$$
$$\xrightarrow{U(\vec{\beta_3},B)} 1/\sqrt{2}\big[|00\rangle - i|11\rangle\big] + 0\big[e^{i\pi/4}|01\rangle + e^{i\pi/4}|11\rangle\big]$$
$$\xrightarrow{U(\vec{\gamma_4},C)} 1/\sqrt{2}\big[|00\rangle + e^{i\pi/4}|11\rangle\big] + 0\big[e^{i\pi/4}|01\rangle + |10\rangle\big]$$
$$\xrightarrow{U(\vec{\beta_4},B)} 1/\sqrt{2}\big[|00\rangle + e^{i\pi/4}|11\rangle\big] + 0\big[e^{i\pi/4}|01\rangle + |10\rangle\big],$$

which is the same final state as before.

V. DISCUSSION

In this paper, we show that ma-QAOA is equivalent to a restriction of dynamic CTQWs in which the underlying graphs can only consist of singletons or of discrete hypercubes with dimension at most n and then find the appropriate operators and angles that yield the universal gate set H, T, and CX in the ma-QAOA framework. Since ma-QAOA

can be viewed as a restriction of dynamic CTQWs, there is potential that well-studied CTQW phenomena, such as hitting times, can be used to determine the optimal β parameters for ma-QAOA. Finding optimal QAOA parameters is a challenging problem, and several techniques such as transferability, reinforcement learning, and neural networks [18–21]. Relating ma-QAOA to CTQWs gives a new framework through which to view the algorithm. It would be of interest to determine if viewing CTQWs through a QAOA lens leads to better understanding of CTQWs.

The authors of [17] gave methods for simplifying dynamic CTQWs based on the underlying graph structure. Since ma-QAOA is equivalent to a restricted dynamic CTQW, ma-QAOA operators can potentially be rearranged and combined to reduce the circuit depth needed to implement arbitrary operations. In the formulation in this manuscript, each H, CX, and T implementation require at most 1.5 layers of ma-QAOA, so a circuit that implements N of these gates would require at most $1.5N$ layers of ma-QAOA. Future work includes examining if there are operations that can be used to reduce the ma-QAOA circuit depth outside of those found in [17].

Finally, in [4], the author proves the universality of QAOA using a line graph quantum architecture, which is not easily comparable to the method of showing ma-QAOA universality in this paper. The author mentions that this architecture is limited but says that the techniques used to prove QAOA universality can be expanded to higher dimensions. It would be of interest to determine if there are cases where the QAOA universality methods in [4] require fewer operations to implement an arbitrary circuit than the method in this paper, and vice-versa. Additionally, fully-connected architecture and gates that act on n qubits for all $n \geq 2$ are required in this implementation, whereas the line architecture in [4] is much more sparse. It would be of interest to determine if there is a more natural method of using QAOA or ma-QAOA for computation on lattices such as the square grid or hexagonal lattice, which more closely model current quantum architecture [22, 23].

[1] Edward Farhi, Jeffrey Goldstone, and Sam Gutmann. A quantum approximate optimization algorithm. *arXiv preprint arXiv:1411.4028*, 2014.

[2] Zhihui Wang, Nicholas C. Rubin, Jason M. Dominy, and Eleanor G. Rieffel. *XY* mixers: Analytical and numerical results for the quantum alternating operator ansatz. *Phys. Rev. A*, 101:012320, Jan 2020.

[3] Andreas Bärtschi and Stephan Eidenbenz. Grover mixers for QAOA: Shifting complexity from mixer design to state preparation. In *2020 IEEE International Conference on Quantum Computing and Engineering (QCE)*, pages 72–82. IEEE, 2020.

[4] Seth Lloyd. Quantum approximate optimization is computationally universal. *arXiv preprint arXiv:1812.11075*, 2018.

[5] Mauro ES Morales, Jacob D Biamonte, and Zoltán Zimborás. On the universality of the quantum approximate optimization algorithm. *Quantum Information Processing*, 19(9):1–26, 2020.

[6] Rebekah Herrman, Phillip C Lotshaw, James Ostrowski, Travis S Humble, and George Siopsis. Multi-angle quantum approximate optimization algorithm. *Scientific Reports*, 12(1):1–10, 2022.

[7] Rebekah Herrman and Travis S Humble. Continuous-time quantum walks on dynamic graphs. *Physical Review A*, 100(1):012306, 2019.

[8] Rebekah Herrman, Lorna Treffert, James Ostrowski, Phillip C. Lotshaw, Travis S. Humble, and George Siopsis. Globally optimizing QAOA circuit depth for constrained optimization problems. *Algorithms*, 14:294, 2021.

[9] Quentin Cappart, Didier Chételat, Elias Khalil, Andrea Lodi, Christopher Morris, and Petar Veličković. Combinatorial optimization and reasoning with graph neural networks. *arXiv preprint arXiv:2102.09544*, 2021.

[10] Kate A Smith. Neural networks for combinatorial optimization: a review of more than a decade of research. *INFORMS Journal on Computing*, 11(1):15–34, 1999.

[11] Edward Farhi and Sam Gutmann. Quantum computation and decision trees. *Physical Review A*, 58:915–928, Aug 1998.

[12] Oliver Mülken and Alexander Blumen. Continuous-time quantum walks: Models for coherent transport on complex networks. *Physics Reports*, 502(2-3):37–87, 2011.

[13] Andrew M Childs and Jeffrey Goldstone. Spatial search by quantum walk. *Physical Review A*, 70(2):022314, 2004.

[14] Andrew M. Childs. Universal computation by quantum walk. *Physical Review Letters*, 102:180501, May 2009.

[15] Thomas G Wong. Isolated vertices in continuous-time quantum walks on dynamic graphs. *Physical Review A*, 100(6):062325, 2019.

[16] K-A Brickman, PC Haljan, PJ Lee, M Acton, L Deslauriers, and C Monroe. Implementation of grover's quantum search algorithm in a scalable system. *Physical Review A*, 72(5):050306, 2005.

[17] Rebekah Herrman and Thomas G Wong. Simplifying continuous-time quantum walks on dynamic graphs. *Quantum Information Processing*, 21(2):1–29, 2022.

[18] Alexey Galda, Xiaoyuan Liu, Danylo Lykov, Yuri Alexeev, and Ilya Safro. Transferability of optimal qaoa parameters between random graphs. In *2021 IEEE International Conference on Quantum Computing and Engineering (QCE)*, pages 171–180. IEEE, 2021.

[19] Ruslan Shaydulin, Phillip C Lotshaw, Jeffrey Larson, James Ostrowski, and Travis S Humble. Parameter transfer for quantum approximate optimization of weighted maxcut. *arXiv preprint arXiv:2201.11785*, 2022.

[20] Matteo M Wauters, Emanuele Panizon, Glen B Mbeng, and Giuseppe E Santoro. Reinforcement-learning-assisted quantum

optimization. *Physical Review Research*, 2(3):033446, 2020.

[21] Guillaume Verdon, Michael Broughton, Jarrod R McClean, Kevin J Sung, Ryan Babbush, Zhang Jiang, Hartmut Neven, and Masoud Mohseni. Learning to learn with quantum neural networks via classical neural networks. *arXiv preprint arXiv:1907.05415*, 2019.

[22] Phillip C Lotshaw, Thien Nguyen, Anthony Santana, Alexander McCaskey, Rebekah Herrman, James Ostrowski, George Siopsis, and Travis S Humble. Scaling quantum approximate optimization on near-term hardware. *Scientific Reports*, 12, 2022.

[23] Alexandru Paler, Simon J Devitt, Kae Nemoto, and Ilia Polian. Mapping of topological quantum circuits to physical hardware. *Scientific reports*, 4(1):1–10, 2014.